Bachelor Thesis

Synthesis and characterization of tetraosmium clusters containing ferrocenyl based diphosphine ligands as potential catalysts in asymmetric hydrogenation

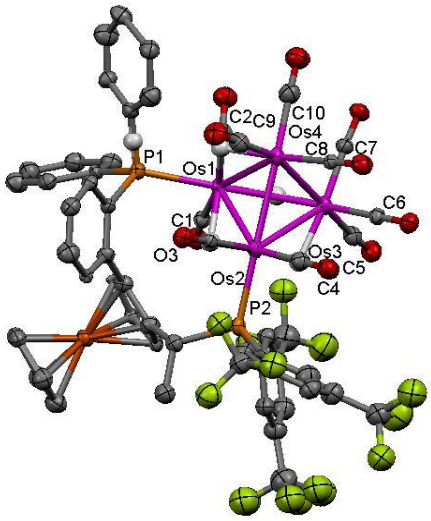

Daniel Svensson

05/27/09 – 11/30/09

Supervisor: Professor Ebbe Nordlander
Advisor: Dr. Abdul Mottalib

Abstract
The metal cluster $[H_4Os_4(CO)_{12}]$ was treated with various chiral ferrocenyl diphosphines of the Walphos family. The new compounds; $[H_4Os_4(CO)_{10}\{\mu$ -1,2-W001$\}]$, $[H_4Os_4(CO)_{10}\{\mu$ -1,2-W002$\}]$, $[H_4Os_4(CO)_{10}\{\mu$ -1,2-W003$\}]$ and $[H_4Os_4(CO)_{10}\{\mu$ -1,2-W005$\}]$ were characterized, and $[H_4Os_4(CO)_{10}\{\mu$ -1,2-W001$\}]$ was investigated in its enantioselective catalytic properties in the hydrogenation of tiglic acid. It was demonstrated that the enantioselectivity with this compound is insignificant (6% ee) and that it is not a suitable hydrogenation catalyst at our conditions (31% conversion).

Introduction
A metal cluster compound is defined as "a finite group of metal atoms that are held together mainly or at least to a significant extent by bonds directly between metal atoms" in 1966 by F. A. Cotton.[1] Metal cluster compounds can be divided into three different groups. The first is the group of so called "naked clusters", or Zintl clusters, for example Pb_5^{2-} and Sn_5^{2-}. The other two groups are the low valence clusters, which is the most common type of metal cluster compounds, and the high valence clusters. High valence metal clusters contains metals in a relatively high oxidation states, usually +2 or +3. These compounds are usually made up of early transition metals and have good π donors as ligands such as chloride, bromide and iodine.
The low-valence clusters on the other hand contain late transition metals with a formal oxidation state of zero or negative. The ligands coordinated to low valence clusters are π -acceptors, and are usually carbon monoxide, but may also be phosphines, a, benzene etc. Due to the fact that the clusters often contain carbon monoxide the low valence clusters are often referred to as metal carbonyl clusters.[3] The smaller covalent metal carbonyl clusters (3-6 metals) are usually electron precise, i.e. they follow the 18 electron rule.[4]

Carbon monoxide and phosphines as ligands
In the present work, transition metal carbonyl clusters have been studied.
The non bonding high lying orbitals that are more or less degenerated in d-block metal complexes are good electron donors and likes to interact with π-acceptors such as carbon monoxide. This can be illustrated by an intermolecular perturbation between ML_5 and CO (Figure 1).

The reason carbon monoxide binds to the metal with the carbon and not the oxygen atom is that the LUMO MO coefficient on carbon is bigger than that on oxygen (this can be explained by electronegativity perturbation).

There are three important consequences of this kind of π-back donation bonding: [5]

- The M-C bond usually gets stronger than that of a metal-ligand bond with a pure σ-donor ligand.
- Because of population of the 2e orbitals (see Figure 1), which have antibonding character with respect to the C-O bond, this bond is weakened and this weakening can be observed as a shifting of the $\nu_{c\text{-}o}$ band towards lower frequencies.
- The electron density on the metal is decreased.

The presence of π -acceptor ligands are essential to the low valence metals. While the bonding of high valence clusters is not significantly affected by donation of some additional electron density to the metals that comes with the covalence of the bonds to ligands, low valence metals with zero such as the osmium metals in this work or negative oxidation state have harder to accept this without the removal of electron density.
Phosphines also function as π-acceptors and σ-donors (Figure 2).

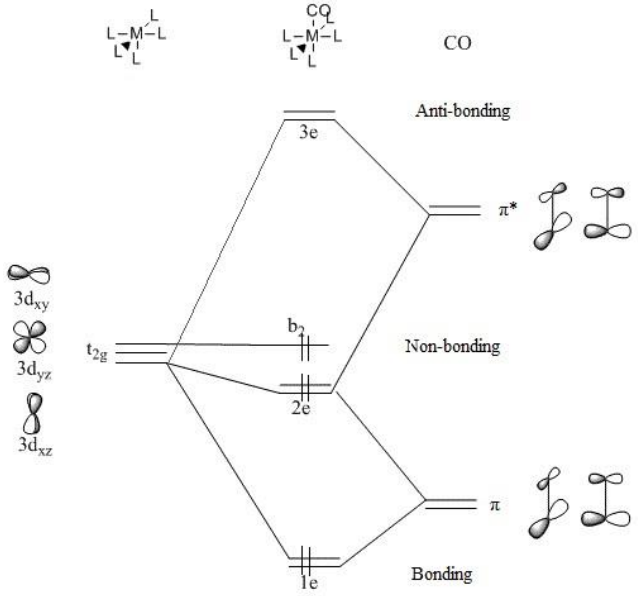

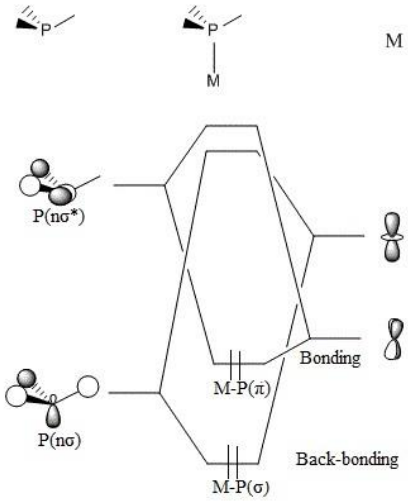

Figure 1. Hoffmann-Albright model of the M-CO bonding Figure 2. Phosphine-Metal bonding

By changing the substituents on the phosphines we can regulate the electon density on the metal. If we have electron-withdrawing groups like fluoride on the phosphine, the π-acceptor strength increases and we get an electron poorer metal.
If we on the other hand put bulky groups on the phosphine the sterics will force the "umbrella" to open up with an increased energy of the phosphine as a consequence. Since the metal frontier orbitals are higher in energy, both the M-P(π) and the M-P(σ) will go up in energy, giving a better σ-donation to the metal making it more electron rich.[5]

The main reason that phosphines are so popular ligands to metal complexes are for their ability to make the metals electron rich. Heterocyclic carbenes also fills this function and can be used instead in many cases, including catalytic hydrogenation. One important difference from the carbenes is that the phosphines have the possibility to go off and on a metal atom, which is necessary in many mechanisms, while the carbenes stay put. The π-back donation to the phosphines also helps stabilizing the clusters, an ability carbenes lack. A drawback with the bulky phosphines are that they are often quite easily oxidized.[5]

Synthesis of the metal clusters

All ligand exchange reactions in this thesis were carried out by oxidative decarboxylation. Previous kinetic studies by Poë and coworkers on $Ru_3(CO)_{12}$ have indicated an associative interchange mechanism which is also possible for the tertiary cluster used here.[2, 6] A substantial bonding of the leaving and incoming ligand in the transition state are characteristic for an interchange mechanism; in an associative interchange (I_a) the bond formation dominates over the bond breaking as opposed to dissociative interchange (I_d) where the bond breaking dominates. In an I_a mechanism the reaction rate shows a dependency on the entering group while in an I_d mechanism the rate only shows a very small dependency on the nature of the entering group.[7] The mechanism is illustrated in Scheme 1.

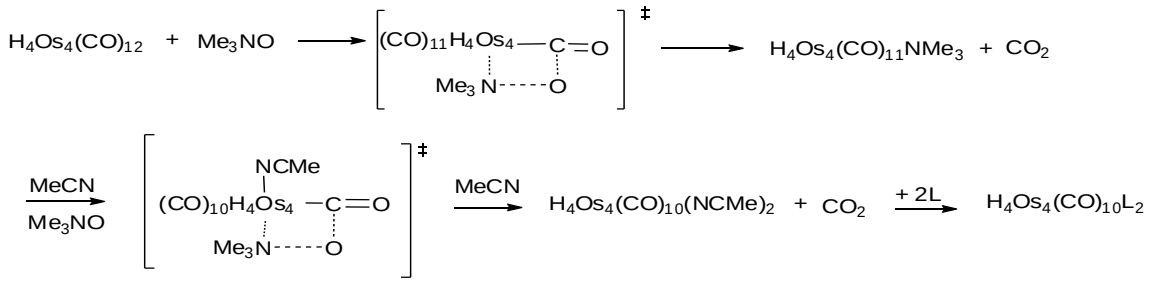

Scheme 1. Proposed mechanism for the oxidative decarbonylation of the metal cluster. L = phosphine.

Interestingly it has been shown that both acetonitrile ligands in $[H_4Os_4(CO)_{10}(NCMe)_2]$ coordinate to the same osmium atom, and not different ones as in $[Os_3(CO)_{10}(NCMe)_2]$.[8]

Diphosphine ligands commonly coordinate to metal clusters in three different fashions, edge bridging (Figure 3:A), chelating (Figure 3:B) and dangling (Figure 3:C). The edge bridging ligands can effectively lock the metal atoms together and thereby maintain cluster nuclearity during reactions.

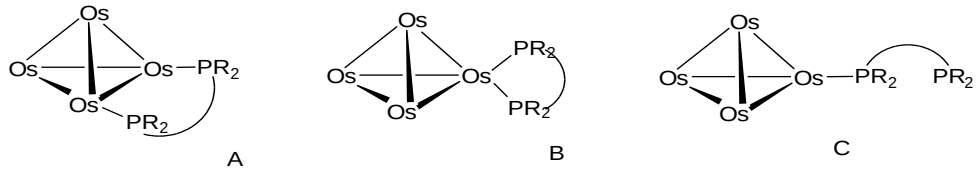

Figure 3. Different common coordination modes of diphosphines to metal clusters

Metal clusters as catalysts

A catalyst is defined as a substance that is not consumed or produced in a reaction but interacts with substrate and products by creating a transition state of lower activation energy and thereby speeding up the reaction kinetics without affecting the thermodynamic equilibrium. This means that it does not make an energetically unfavoured reaction possible but speeds up reactions that are possible. Over 90% of all industrial chemical synthesis is done by the help of catalysis; this includes pharmaceutical manufacturing, fuel production etc. [9]

Catalysts are often based on transition metals due to their ability to bind a wide variety of molecules. The catalysis of chemical processes is divided into two fields, homogeneous catalysis where the catalyst is dissolved in the same phase as the substrate and heterogeneous catalysis where the catalyst is a solid. Heterogeneous catalysts, which are often prepared by adding the catalytic metal on a supporting material so that a layer of catalyst is formed, are less easily manipulated than homogenous catalysts but have the great advantage of higher thermal stability, which allows for high temperature and pressure reactions. The surface materials can also catalyze reactions that require cooperative effects between several metal atoms, which are not possible by simple homogenous metal catalysts.

Using metal clusters in homogeneous catalysis is of great interest since they, in principle, have the advantage of cooperative effects between several metal atoms but also allow for manipulation of selectivity and reactivity by ligand design. Manipulating the steric and electronic properties of the ligands on the metal cluster makes it possible to achieve size selectivity, e.g. branched or linear products and the selective preparation of one enantiomer, the latter being called asymmetric synthesis. For asymmetric synthesis chiral ligands are usually used, which in the ideal reaction can transfer their chirality to the product.

In addition to their potential as catalysts in their own right, transition metal clusters have also been used as models for catalytic metal surfaces. The similarities between the metal surfaces in heterogeneous catalysis and clusters in homogenous catalysis are many. The organization of the metal atoms in clusters is often similar to the configuration of the bulk crystals and they also have energetic, electronic and vibrational properties in common. This has made the analogy of using metal clusters as models of surface catalysis popular. This analogy, commonly referred to as the 'cluster-surface analogy', was probably first suggested by Burwell and then firmly established in reviews made by Muetterties.[6, 10] There are however a few important differences. One is that bulk crystals have the presence of free adsorption sites that can increase the reactivity. In other words the model is simplified when it comes to interaction between the substrate and metal. The advantage of using clusters as surface models is that the mechanism of the catalyzed reactions can be studied in solution, using clusters of the metal instead of a solid phase, which allows for common spectroscopic methods such as IR, NMR and UV-VIS.

Closely related compounds to the new compounds synthesized in this thesis have been shown to catalyze a range of asymmetric reactions. For example clusters of the same general formula as the new compounds but with ruthenium instead of osmium, $[H_4Ru_4(CO_{12-2n}(P\text{-}P)x]$ (x = 1,2, P-P = chiral diphosphine), have been shown to catalyze many different asymmetric reactions such as hydroformylation, isomerisation and hydrogenation.[2] The chiral diphosphines used in this thesis are of the Walphos family (Figure 4), which has been proven to give high enantioselectivity in mononuclear rhodium and ruthenium based hydrogenation.[2]

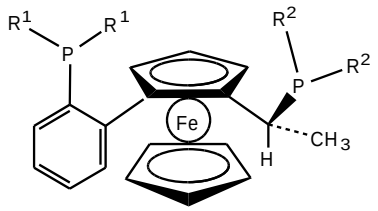

Figure 4. General structure for the Walphos ligands

My focus has also been on the hydrogenation using the substrate tiglic acid (Scheme 2). Asymmetric hydrogenation is a process which cannot be done by any other means than homogenous catalysis. The hydrogenation was done by H_2, which is one of several known methods for hydrogenation. Hydrogenation of tiglic acid is a good bench mark reaction for assymetric hydrogenation, as the substrate is prochiral, which means that it can be converted into a chiral molecule in one step. Furthermore it is not very bulky, which, as previously discussed, can be a problem with the cluster catalysts as the ligands can block access of the bulky substrates to the metal center.

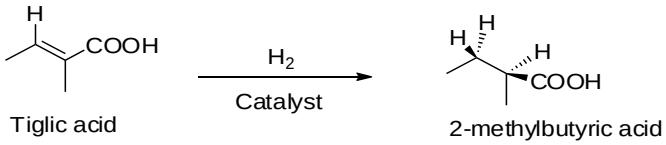

Scheme 2. Catalyzed hydrogenation of tiglic acid

Mechanism of the catalytic reactions

The mechanism of the reaction of cluster complexes is difficult to determine due to the great number of possible mechanisms that has to be eliminated to leave only one route. Another problem with determining the catalytic mechanism is that the complexes involved in the catalytic cycle are often present in too low concentrations for detection by spectroscopic methods. Also the catalyst added might not be involved in the actual catalytic steps but may be a precursor for the active components. It is probably so that we do not yet know beyond reasonable doubt the mechanism for any cluster catalyzed reactions, but there are now sensible proposals for many of them. [10]

It is a difficult problem to prove that catalysis does not occur after fragmentation of the cluster to mononuclear complexes followed by homogenous catalysis by simple organometallics, or even by association to larger metal particles followed by heterogeneous catalysis. Even stable clusters like $[Ru_3(CO)_{12}]$ react by addition of CO and fragmentation of metal-metal bonds under conditions commonly used for catalytic carbonylation reactions. In this case $[Ru(CO)_5]$ is formed which is known to be an active homogenous catalyst. Others clusters often undergo thermal ligand loss and the aggregation that follows give higher clusters or metal particles which can induce heterogeneous catalysis. There is no simple test to exclude this and a combination of qualitative tests and detailed kinetic studies are needed. One commonly used method to avoid heterogeneous catalysis is mercury poisoning. By addition of metallic mercury transition metal particles forms inactive amalgams. Kinetic or product selectivity studies are the usual way to test for fragmentation. [2]

In the case of tetraruthenium clusters with diphosphine ligands a correlation between the enantioselectivity in hydrogenation and the hydride fluxionality has been seen in previous work.[11] Catalysts such as $[H_4Ru_4(CO)_{10}$-{μ -1,2-DIPAMP}], which has fluxional hydrides at room temperature (only one hydride signal in ^{1}H NMR), only exhibit poor enantioselectivity. On the other hand, in enantioselective hydrogenation catalysts such as $[H_4Ru_4(CO)_{10}$(P-P)], with P-P being Walphos 001 and 002 (Figure 5) in different coordination modes, the hydrides are not fluxional at room temperature and thereby give rise to sharp resonances at distinct shift. When raising the temperature to 110 °C, three of the four hydrides becomes fluxional while the fourth hydride, which is the one bridging the Ru-Ru edge, remains fixed. This has lead to the hypothesis

that transfer of this hydride may be responsible for the enantioselectivity.[2] Kinetic studies such as these has made it possible for Viktor Moberg to propose a mechanism for the hydrogenation reaction of tiglic acid by $[H_4Ru_4(CO)_{10}\{\mu\text{-}1,2\text{-walphos}\}]$.[2] Here this mechanism is expressed in Scheme 3 as the osmium equivalent studied in this paper.

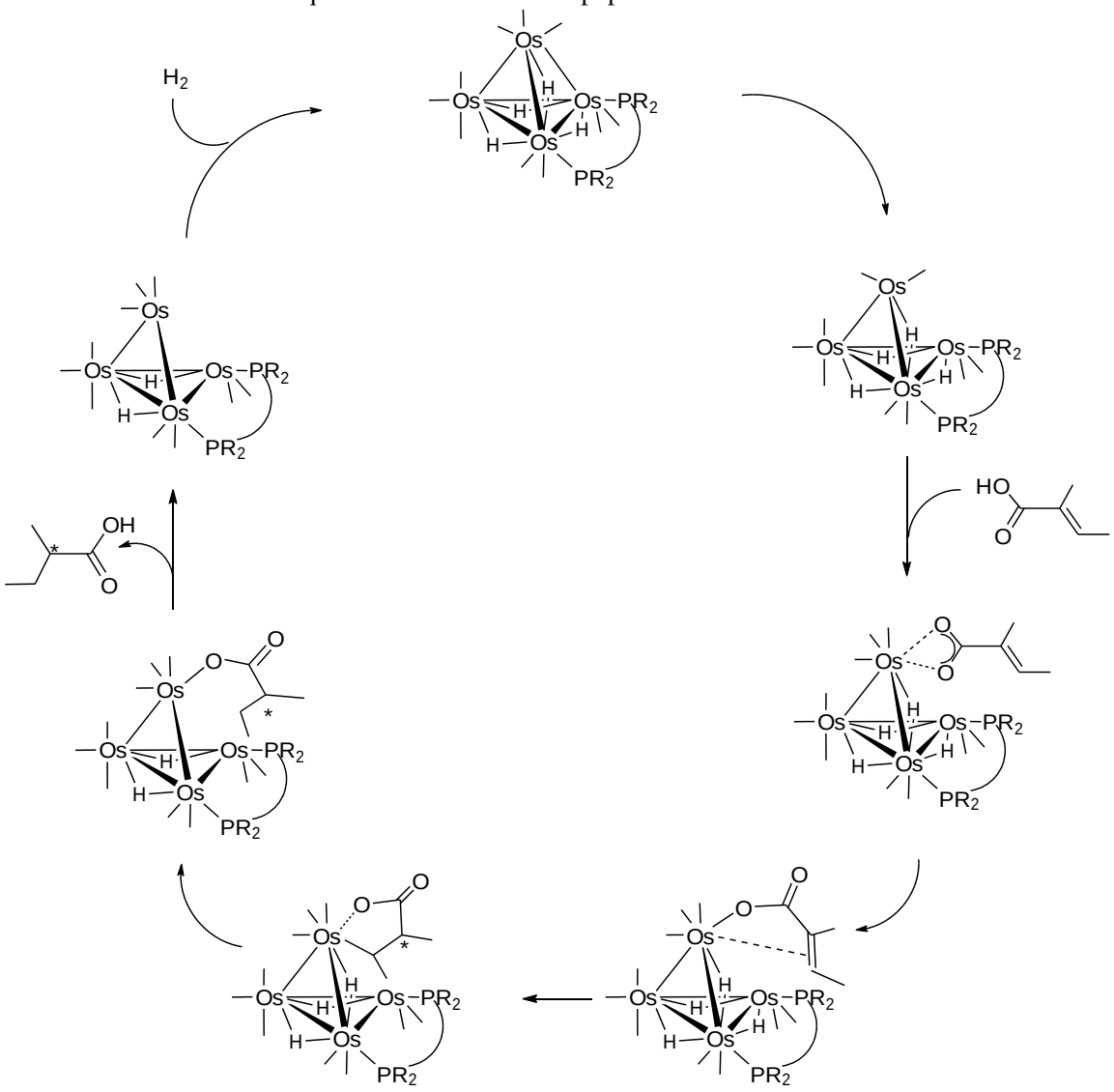

Scheme 3. Proposed reaction mechanism for the catalytic hydrogenation of tiglic acid. The initial step is a heterolytic metal-metal bond rupture to form an unsaturated 60-electron 'butterfly-cluster structure' followed by coordination of substrate to form a metal-carboxylate chelate complex. The hydrides hydrogenate the substrate in two step where the first is supposedly stereo selective. The formed carboxylate serves as a base, activating protonated substrate. The hydrides are regenerated by addition of H_2 and the cycle is completed by the formation of a metal-metal bond.

Experimental

General procedures

All reactions were carried out under nitrogen atmosphere using standard Schlenk techniques. Isolation of the products where done by preparative TLC without exclusion of air. $[H_4Os_4(CO)_{12}]$ was obtained from the supervisor and the Walphos ligands where acquired from commercial

sources. ^{1}H and ^{31}P NMR spectra were obtained using a Varian Inova 500MHz at 25º C. IR spectra where recorded using an Avatar 360 FT-IR spectrometer.

Synthesis of $[H_4Os_4(CO)_{10}\{\mu$ -1,2-W001$\}]$ (1)

$[H_4Os_4(CO)_{12}]$ (50 mg, 45 μmol) was added to a 100 ml round bottom flask with gas inlet and a stirring bar. The flask was connected to a Schlenk line and flushed with nitrogen. After addition of 10 mL dry MeCN to the flask a 100 mL pressure equalized addition funnel was connected. The entire system was flushed with nitrogen for a few minutes after which a solution of $Me_3NO{\cdot}2H_2O$ (10 mg, 93 μmol) dissolved in 9 mL MeCN was added to the addition funnel. The addition funnel was closed by a stopper and the acetonitrile solution was added drop wise to the yellow solution under vigorous stirring over a period of 30 minutes at which the yellow colour darkened. After an additional hour of stirring at room temperature most of the solvent was removed in vacuo leaving brown viscous liquid.

To this liquid, 15 mL of dichloromethane was added along with 1.3 equivalents of SL-W001-1 ligand (55 mg, 59 μmol). A working condenser was connected and the entire system flushed with nitrogen for a few minutes while stirring vigorously after which the mixture was left for reflux for two hours in a water bath.

Most of the solvent was removed in vacuo and purified using preparative TLC (Merck Kiselgel 50, eluent 1:1 dichloromethane:n-hexane). Unreacted ligand could be recovered as a band at the solvent front (8.4 mg, 9 μmol). The major product, $[H_4Os_4(CO)_{10}\{\mu$ -1,2-W001$\}]$ (1), was isolated around Rf 0.6 (31.5 mg, 16 μmol, 32%) giving orange crystals after recrystallization from hexane/dichloromethane at -20 ºC. IR (νCO, dichloromethane): 2075 m, 2063 w, 2050 m, 2030 s, 2009 s, 1991 m, 1962 w cm^{-1}. ^{1}H NMR ($CDCl_3$): δ 8.39 (m, 1H), 8.14 (s, 1H), 7.87 (s, 1H), 7.77 (d, J=9.00, 2H), 7.73 (s, 1H), 7.71 (s, 1H), 7.68 (s, 3H), 7.61 (m, 2H), 7.53 (m, 1H), 7.45 (m, 4H), 7.31 (t, J=7.3, 1H), 7.25 (s, 1H), 7.17 (m, 1H), 4.01 (s(m), 1H, cp), 3.92 (s, 5H, cp), 3.91 (s, 1H, cp) 3.75 (s, 1H, cp), 3.55 (m, 1H, CH), 1.75 (dd, J = 11.73, J = 7.12, 3H, CH3), -18.9 (d, J = 14.4, 1H), -19.16 (d, J = 8.5, 1H), -19.82 (d, J = 19.7, 1H), -20.17 (t, J = 9.56, 1H). ^{31}P NMR ($CDCl_3$): δ 15.36 (s), 0.39 (s). MS (FAB+): *m/z* 1968.

Synthesis of $[H_4Os_4(CO)_{10}\{\mu$ -1,2-W002$\}]$ (2)

$[H_4Os_4(CO)_{12}]$ (52 mg, 47 μmol) was added to a 100 mL round bottom flask with gas inlet and a stirring bar. The flask was connected to a Schlenk line and flushed with nitrogen. After addition of 10 mL dry MeCN to the flask a 100 mL pressure equalized addition funnel was connected. The entire system was flushed with nitrogen for a few minutes after which a solution of $Me_3NO{\cdot}2H_2O$ (11 mg, 102 μmol) dissolved in 9 mL MeCN was added to the addition funnel. The addition funnel was closed by a stopper and the acetonitrile solution was added drop wise to the yellow solution under vigorous stirring over a period of 10 minutes at which the yellow colour darkened. After an additional hour of stirring at room temperature most of the solvent was removed in vacuo leaving a brown viscous liquid. To this 10 mL of dichloromethane was added along with just over 1 equivalent of SL-W002-1 ligand (33 mg, 50 μmol). A working condenser was connected and the entire system flushed with nitrogen for a few minutes while stirring vigorously after which the mixture was left for reflux for two and a half hours in water bath.

Most of the solvent was removed in vacuo and purified using preparative TLC (Merck Kiselgel 50, eluent 1:1 dichloromethane:n-hexane). Unreacted ligand could be recovered as a band at the solvent front (6 mg, 9 μmol). The major product, $[H_4Os_4(CO)_{10}\{\mu$ -1,2-W002$\}]$ (2), was isolated as a orange solid around Rf 0.86 (6 mg, 3.5 μmol, 7.5%). IR (νCO, dichloromethane): 2074 s, 2058 s, 2010 vs, 1986 s, 1956 w, 1942 cm^{-1}. ^{1}H NMR ($CDCl_3$): δ 8.39 (dd, J = 7.51, J = 4.93, 1H), 7.62 (t, J = 5.62, H=2), 7.58 (s, 1H), 7.56 (s, 1H), 7.54 (d, J = 7.47, 2H), 7.52 (s, 1H), 7.50 (s, 2H), 7.47 (m, 6H), 7.44 (s, 1H), 7.42 (s, 1H), 7.40 (s, 1H), 7.39 (m, 2H), 7.31 (m, 2H), 7.24 (t,

J= 7.87, 1H), 4.00 (s, 1H, cp), 3.82 (s, 5H, cp), 3.75 (s, 1H, cp), 3.38 (s, 1H, cp), 2.55 (br, 1H, CH), 1.82 (dd, J = 11.72, J = 7.09, 3H, CH3), -19.29 (d, J=11.56, 1H), -19.41 (d, J = 5.89, 1H), -19.43 (d, J = 9.43, 1H), -19.57 (d, J = 4.25, 1H). ^{31}P NMR ($CDCl_3$): δ 17.68 (s), 6.55 (s). MS (FAB+): *m/z* 1704.

Synthesis of [$H_4Os_4(CO)_{10}${μ -1,2-W003}] (3)

[$H_4Os_4(CO)_{12}$] (50 mg, 45 μmol) was added to a 100 mL round bottom flask with gas inlet and a stirring bar. The flask was connected to a Schlenk line and flushed with nitrogen. After addition of 10 mL dry MeCN to the flask a 100 mL pressure equalized addition funnel was connected. The entire system was flushed with nitrogen for a few minutes after which a solution of $Me_3NO{\cdot}2H_2O$ (10 mg, 93 μmol) dissolved in 9 mL MeCN was added to the addition funnel. The addition funnel was closed by a stopper and the acetonitrile solution was added drop wise to the yellow solution under vigorous stirring over a period of 30 minutes at which the yellow colour darkened. After an additional hour and a half of stirring at room temperature most of the solvent was removed in vacuo leaving brown viscous liquid. To this 10 mL of dichloromethane was added along with just over 1 equivalent of SL-W003-1 ligand (33 mg, 50 μmol). A working condenser was connected and the entire system flushed with nitrogen for a few minutes while stirring vigorously after which the mixture was left for reflux for two hours in water bath.

Most of the solvent was removed in vacuo and purified using preparative TLC (Merck Kiselgel 50, eluent 1.5:2 dichloromethane:n-hexane). [$H_4Os_4(CO)_{10}${μ -1,2-W003}] (3) was isolated as a orange solid at Rf 0.7 (6 mg, 3.5 μmol, 7.8%). IR (vCO, dichloromethane): 2075 m, 2056 s, 2021 vw, 2005 vs, 1982 m, 1930 vw cm^{-1}. ^{1}H NMR ($CDCl_3$): δ 8.40 (m, 1H), 8.19 (dd, J = 4.79, J = 6.75, 1H), 7.63 (s, 2H) 7.60 (m, 2H), 7.44 (t, 7.58, 2H), 7.35 (br, 3H), 7.21 (t, J = 7.22, 2H), 6.45 (t, J =9.03, 1H), 4.14 (s, 1H, cp), 4.00 (s, 1H, cp), 3.92 (s, 5H, cp), 3.46 (s, 1H, cp), 3.40 (t, J = 7.42, 1H, CH), 2.27 (dd, J = 9.62, J = 7.61, 3H, CH3), 1.89-1.57 (m, 13H, cy), 1.40-1.27 (m, 9H, cy), -19.06 (d, J = 11.57, 1H), -19.57 (s, 1H), -19.98 (t, J = 8.84, 1H), -20.36 (d, J = 6.85, 1H). ^{31}P NMR ($CDCl_3$): δ 31.00 (d, J=24.48), 5.44 (s). MS (FAB+): *m/z* 1714.

A one pot synthesis with the same quantities used above where also performed by adding the ligand and cluster directly to the flask along with 15 ml dichloromethane. After dripping in the $Me_3NO{\cdot}2H_2O$ solution (9 ml MeCN) the reaction mixture was refluxed for 3 hours. Some [$H_4Os_4(CO)_{10}${μ -1,2-W003}] (3) could be isolated (3 mg, 1.8 μmol, 4%).

Synthesis of [$H_4Os_4(CO)_{10}${μ -1,2-W005}] (4)

[$H_4Os_4(CO)_{12}$] (53 mg, 48 μmol) was added to a 100 mL round bottom flask with gas inlet and a stirring bar. The flask was connected to a Schlenk line and flushed with nitrogen. After addition of 10 mL dry MeCN to the flask a 100 mL pressure equalized addition funnel was connected. The entire system was flushed with nitrogen for a few minutes after which a solution of $Me_3NO{\cdot}2H_2O$ (10 mg, 93 μmol) dissolved in 9 mL MeCN was added to the addition funnel. The addition funnel was closed by a stopper and the acetonitrile solution was added drop wise to the yellow solution under vigorous stirring over a period of 18 minutes at which the yellow colour darkened. After an additional two hours and ten minutes of stirring at room temperature most of the solvent was removed in vacuo leaving brown viscous liquid.

To this a suitable amount of dichloromethane was added along with just over 1 equivalent of SL-W005-1 ligand (51 mg, 49 μmol). A working condenser was connected and the entire system flushed with nitrogen for a few minutes while stirring vigorously after which the mixture was left for reflux for two hours in water bath.

Most of the solvent was removed in vacuo and purified using preparative TLC (Merck Kiselgel 50, eluent 1:1 dichloromethane:n-hexane). [$H_4Os_4(CO)_{10}${μ -1,2-W005}] (4) was isolated as a orange solid at Rf 0.4 (5 mg, 2.4 μmol, 5%). IR (vCO, dichloromethane): 2074m, 2049m, 2030s, 2008s, 1990w, 1962w cm^{-1}. ^{1}H NMR ($CDCl_3$): δ 8.38 (dd, J= 7.66, J = 5.10, 1H), 8.13 (s, 1H), 7.85 (s, 1H), 7.68 (t, J = 9.20, 4H), 7.58 (t, J = 7.62, 2H), 7.28 (t, J = 7.78, 4H), 7.21 (dd, J= 8.02,

J = 13.41, 1H), 3.91 (s, 5H, cp), 3.89 (s, 1H), 3.87 (s, 3H), 3.83 (s, J=2.69, 1H), 3.79 (s, 1H), 3.77 (s, 3H), 3.61 (s, 1H), 2.43-2.28 (m, 12H), 1.70 (dd, J= 7.09, J = 11.76, 3H), -18.92 (d, J= 14.94, 1H), -19.27 (d, J = 8.76, 1H), -19.85, (d, J = 23.13, 1H), -20.47 (t, J = 9.45, 1H). ^{31}P NMR ($CDCl_3$): δ 14.63 (s), -2.63 (s). MS (FAB+): *m/z* 2092.
A one pot synthesis with the same quantities used above where also performed by adding the ligand and cluster directly to the flask along with 20 mL dichloromethane. After dripping in the $Me_3NO{\cdot}2H_2O$ solution (10 ml MeCN) the reaction mixture was refluxed for 4 hours. Some $[H_4Os_4(CO)_{10}\{\mu\text{-}1,2\text{-}W005\}]$ (4) could be isolated as the third band (8.2 mg, 3.9 μmol, 8.2%) giving orange crystals after recrystallization from n-hexane/dichloromethane at -20 ºC.

Catalytic experiment with $[H_4Os_4(CO)_{10}\{\mu\text{-}1,2\text{-}W001\}]$ (1)
An autoclave was loaded with $[H_4Os_4(CO)_{10}\{\mu\text{-}1,2\text{-}W001\}]$ (10.8 mg, 55 μmol) and tiglic acid in a hundred fold excess as substrate (55 mg, 5.5 mmol) along with a degassed solvent mixture (2.5 mL EtOH/2.5 mL toluene). The reaction vessel was closed and purged two times with hydrogen before final pressurizing to 50 bars. The reaction mixture was heated to 100 ºC under stirring (600 rpm) for 24 hours. After this the autoclave was left to cool for approximately one hour before the vessel was carefully depressurized and opened. The reaction mixture was transferred to a flask and the solvent removed in vacuo. The reaction mixture was dissolved in Et_2O (5 mL) and the carboxylic acid was extracted with a $NaHCO_3$ solution (sat. 3×10 mL) and the catalyst was recovered from the yellow ether phase by TLC (4 mg, 37%). The $NaHCO_3$ phase was then washed with Et_2O (2×5mL) and protonated by dripping in conc. H_2SO_4 in the mixture until neutral. The carboxylic acid was extracted with Et_2O (3×10 mL) and washed with H_2O (2×5 mL). The ether phase was dried over Na_2SO_4, filtered and evaporated in vacuo yielding light yellow oily crystals (43 mg). The conversion was calculated from the ^{1}H NMR spectra of the product, by integration of the triplet and doublet from the product at 0.95 and 1.18 respectively and compare to the singlet at 1.84 from the unreacted acid (30.56% conversion).

The enantiomeric excess of the product was determined by conversion of the reduced tiglic acid with (S)-methyl mandelate and analyzing the diastereomeric mixture by ^{1}H NMR. The reaction was run under an excess of reagent by assuming 40% conversion. The obtained yellow crystals (43 mg, 40% yield, 0.166 mmol) was dissolved in 1 mL of dichloromethane and added to a 25 mL three neck flask equipped with stirring bar and septum. The flask was flushed with nitrogen and cooled to -10 °C. 4-dimethyaminopyridine (1 mg) dissolved in 0.5 mL dichloromethane was added by syringe under stirring followed by methyl (S)-(+)-mandelate (20.3 mg, 0.166 mmol) in 0.5 mL dichloromethane and N,N-dicyclohexylcarbodiimide (34.3 mg, 0.166 mmol) in 0.5 mL dichloromethane. The milky reaction mixture was stirred for 3 hours at around -10 °C after which the precipitated dicyclohexylurea was filtered of and the solvent removed in vacuo yielding white crystals (58 mg). ^{1}H NMR of the product (Figure 5) revealed the enantiomeric excess, each enantiomer gives rise to one singlet, one doublet and one triplet which can be compared by integration.

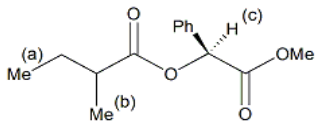

Figure 5. (S)-methyl mandelate derivative of tiglic acid. The ^{1}H NMR assignment in table below.

Table 1. ^{1}H NMR assignment of (S)-methyl mandelate derivative of tiglic acid

Assignation	Multiplicity	(S-S) isomer	(R-S) isomer
H(a)	Triplet	0.98	0.92
H(b)	Doublet	1.19	1.24

H(c)	Singlet	5.93	5.97

The enantiomeric excess was calculated by the equation % ee = ((S-R)/(R+S))×100. Integration of the triplets gave 1 to (S-S) and 0.88 to (R-S) so the enantiomeric excess was 6.4% in the above reaction.

Catalytic experiment with $[H_4Os_4(CO)_{12}]$ was carried out exactly as above, using 10 mg of cluster and 90.3 mg of tiglic acid. Some catalyst could be recovered. No conversion was noticed.

A yellow decomposition product recovered as a low band at all reactions (IR: 2080 m, 2050 vs, 2020 vs, 1998 s, 1979 m, No P, MS (FAB+): *m/z* 473) where also tested was also tested (14.4 mg, 7.3 μmol and 74 mg tiglic acid). No catalyst could be recovered, and no conversion of tiglic acid was noticed.

Results and discussion

Four different ligands of the Walphos family (Figure 6) where used as precursors.

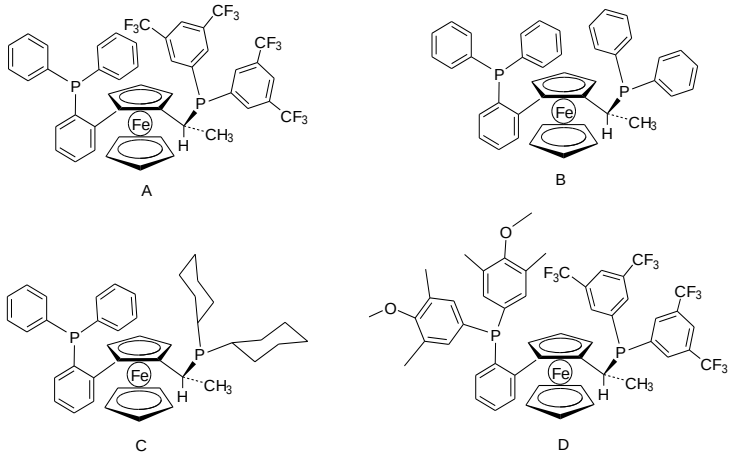

Figure 6. Walphos ligands used, A (R)-(R)-W001, B (R)-(R)-W002, C (R)-(R)-W003, D (R)-(R)-W005

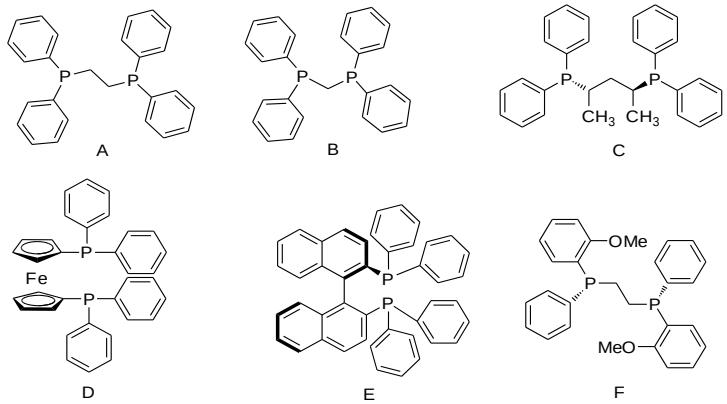

Figure 7. Other diphosphine ligands discussed in this thesis: A DPPE, B DPPM, C (S,S)-DBPP, D DPPF, E (R)-BINAP, F (R,R)-DIPAMP

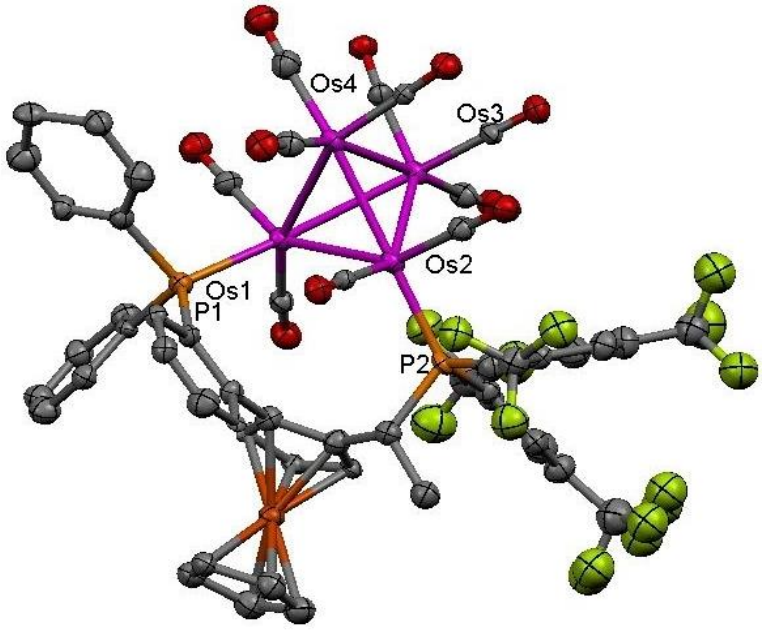

Figure 8. ORTEP plot of the molecular structure of $[H_4Os_4(CO)_{10}\{\mu\text{-}1,2\text{-}W001\}]$ (1). Selected bond lengths (Å) and angles (deg): Os(1)-Os(4) 3.009, Os(1)-Os(2) 3.029, Os(1)-Os(3) 3.031, Os(2)-Os(4) 2.794, Os(2)-Os(3) 2.941, Os(3)-Os(4) 2.802, Os(1)-P(1) 2.375, Os(2)-P(2) 2.324, P(1)-Os(1)-Os(2) 107.70, P(1)-Os(1)-Os(3) 161.78, P(2)-Os(2)-Os(1) 116.29, P(2)-Os(2)-Os(3) 119.40.

In the molecular structure of $[H_4Os_4(CO)_{10}\{\mu\text{-}1,2\text{-}W001\}]$ (1) two Os-Os bonds are significantly shorter than the starting cluster, while the rest are longer or approximately the same.[12] One of the shorter Os-Os bonds, which is from the osmium connected to a phosphorus, can be explained by the asymmetric increase of electron density on the metal that comes with the phosphine.[13] The Os-Os bond that is next to the other phosphorus is slightly shorter than it was in the starting cluster. The second bond that is significantly shorter, is between the two osmium atoms that are not connected to any phosphine. While this cannot be readily explained, it agrees with the binding pattern in related clusters, such as $[H_4Ru_4(CO)_{10}\{\mu\text{-}1,2\text{-}(R)\text{-}W001\}]$, $[H_4Ru_4(CO)_{10}\{\mu\text{-}1,2\text{-}(R)\text{-}W002\}]$[3], $[H_4Ru_4(CO)_{10}\{\mu\text{-}1,2\text{-}(R,R)\text{-}BDPP\}]$[14] and $[H_4Os_4(CO)_{10}\{\mu\text{-}1,2\text{-}DPPF\}]$[8]. In the nine-membered ring one phosphorus atom (P1) coordinates in an equatorial position while the second (P2) coordinates in an axial position. This very unusual coordination mode of diphosphine ligands on tetrahedral cores have previously been observed for Walphos ligands coordinated to H_4Ru_4 clusters.[15]

Determining the coordination mode of the ligand to the cluster has been a bit problematic due to the lack of good crystals. It is likely that the kinetic product is the chelating one and the bridging is the thermodynamic product. This conclusion is based on the fact that the large rings (here 9 atoms) formed should prefer a bridging coordination mode, while the crowded smaller rings have been shown to have the chelating product as the thermodynamically favored product and the bridged product as the kinetically favoured.[16, 17]
It has also been strongly suggested, but not confirmed, that when the chelating cluster formed in the reaction between W001 and $[(\mu\text{-}H)_3Ru_3Rh(CO)_{12}]$ is heated to 110 °C the cluster converts to the bridging isomer,[11] just as with the $[Os_3(CO)_{12}]$ + DPPF products.[17] The opposite is true for more crowded ligands; $[H_4Ru_4(CO)_{10}\{\mu\text{-}1,2\text{-}P\text{-}P\}]$ rearranges to the thermodynamically favored $[H_4Ru_4(CO)_{10}\{\mu\text{-}1,1\text{-}P\text{-}P\}]$ when P-P being DPPE[18], BDPP[14], BINAP[19], and DIPAMP[20] upon heating.

Two indications of the coordination mode can be the following:
1. The bridging complex should elute faster on silica than the chelating with dichloromethane/n-hexane as solvent.[21]
2. Due to the large nuclear deshielding of chelating diphosphine ligands the chelating clusters should give a high shift in ^{31}P NMR while the bridging cluster that binds to adjacent osmium atoms should give a low shift (often negative).[16]
In the experiments described above the reactions only give one major product along with some side products, either apparent decomposition products, or products of too low yield to run NMR analysis. This has made the first point less important than the second. In the case of $[H_4Os_4(CO)_{10}\{\mu$ -1,2-W001$\}]$ crystallography confirmed bridging coordination. The ^{31}P NMR shifts of that compound shows one singlet at δ 15 and one at around δ 0. This fits quite well with the other major Walphos products ^{31}P shifts (W002 = δ 18 (s), 7(s), W003 = δ 31(s), 5(s), W005 = δ 14 (s), -3 (s)).

The only diphosphine cluster studied in its catalytic properties in hydrogenation was $[H_4Os_4(CO)_{10}\{\mu$ -1,2-W001$\}]$. The reaction was carried out under 50 bar of H_2 pressure at 100 °C and the results showed 31% conversion of tiglic acid and 6% enantiomeric excess (S-configuration). These results are significantly worse than those obtained for analogous H_4Ru_4 clusters, but it was an improvement from the starting cluster $[H_4Os_4(CO)_{12}]$, which did not give any noticeably conversion at the same conditions. The latter observation was somewhat suprising since $[H_4Os_4(CO)_{12}]$ has previously been shown to catalyze the hydrogenation of styrene.[22] The reason for the lack of observation of any hydrogenation catalysis could be the milder conditions used in my experiments.

Kinetic studies of the fluxionality of the hydrides would be of interest to see how the present $[H_4Os_4(CO)_{10}$(P-P)] clusters differ from the analogous ruthenium based catalysts which shows good activity.

The yield of the products were relatively low. The highest yield was 32% of $[H_4Os_4(CO)_{10}\{\mu$ -1,2-W001$\}]$, but in the other reactions the yields where significantly lower (around 10%). There generally did not seem to be any great difference in terms of yield or distribution of the major products when ligand and starting cluster were mixed from the beginning (one-pot) and the other method in which the cluster first is reacted with Me_3NO/MeCN before the ligand was added (even though the highest yield was achieved by the second method). The observed catalytic efficiency is very poor in comparison to the ruthenium analogue of the above-mentioned cluster. This is in keeping with the relative strengths of metal-metal and metal-carbonyl bonds in osmium clusters relative to their ruthenium analogues; both kinds of bonds are stronger, making osmium clusters less reactive than analogous ruthenium clusters under equivalent reaction conditions.

Conclusion

Activation of the tetraosmium cluser $[H_4Os_4(CO)_{12}]$ with Me_3NO in the presence of different chiral ferrocenyl diphosphines yielded the new compounds $[H_4Os_4(CO)_{10}\{\mu\text{-}1,2\text{-}W001\}]$, $[H_4Os_4(CO)_{10}\{\mu\text{-}1,2\text{-}W002\}]$, $[H_4Os_4(CO)_{10}\{\mu\text{-}1,2\text{-}W003\}]$ and $[H_4Os_4(CO)_{10}\{\mu\text{-}1,2\text{-}W005\}]$. These chiral clusters were fully characterized by IR and NMR spectroscopies and the molecular structure of $[H_4Os_4(CO)_{10}\{\mu\text{-}1,2\text{-}W001\}]$ were determined by X-ray crystallography. The enantioselective catalytic property of $[H_4Os_4(CO)_{10}\{\mu\text{-}1,2\text{-}W001\}]$ were also studied in the hydrogenation of tiglic acid at which it showed poor results (6% ee at 31% conversion) as opposed to the corresponding ruthenium clusters which has shown far superior results in previous works. The reaction conditions and product isolation of the ligand substitution could be worth optimizing in further work to improve the yields.

Acknowledgments

I would like to thank my supervisor, Professor Ebbe Nordlander, for offering me the possibility to work in this project and my other advisor, Dr. Abdul Mottalib, for all the help.
I would also like to thank Dr. Matti Haukka of the University of Joensuu in Finland for doing the X-ray diffraction studies of my crystals.

References

(1) F.A Cotton, *Quarterly reviews* 1966, 20, 389
(2) V. Moberg, *Cluster-Based Catalysts for Assymetric Synthesis* 2007, 3-30
(3) V. Moberg, M. Haukka, I. O. Koshevoy, R. Ortiz and E. Nordlander, *Organometallics* 2007, 26, 4090-4093
(4) G. L. Geoffry, B. F. G. Johnson and Robert, *Topics in Inorganic and Organometallic Stereochemistry Volume 12*, 1981, 264-274
(5) K. J. Szabó Handouts for KO7007 based on T. Albright *Orbital Interactions in Chemistry*
(6) B. Ambwani, S. K. Chawla and A. J. Poë, *Kinetics of associative reactions of* $Ru_3(CO)_{10}(\mu$-*dppm)* 1988
(7) C. E. Housecroft, *Inorganic Chemistry* 2007, 882
(8) Y.-Y. Choi and W.-T. Wong, *Journal of Organometallic Chemistry* 542 (1997), 121-129
(9) Jens Hagen, *Industrial catalysis: a practical approach* (2006)
(10) L. A. Oro, P. Braunstein and P. R. Raithby, *Metal Clusters in Chemistry Volume 2: Catalysis and Dynamics and Physical Properties of Metal Clusters* 1999
(11) A. M. Mottalib, Unpublished results
(12) B. F. G. Johnson, J. Lewis, P. R. Raithby and C. Zuccaro, *Acta Crystallography* (1981). B37, 1728-1731
(13) V. Moberg, A. M. Mottalib, D. Sauer, Y. Poplavskaya, D.C. Craig, S.B. Colbran, A.J. Deeming and E. Nordlander, *Chiral and achiral phosphine derivatives of tricobalt carbyne clusters as catalyst precursors for (assymetric) inter- and intramolecular Pauson-Khand reactions* (manuscript)
(14) P. Homanen, R. Persson, M. Haukka, T. Pakkanen and E. Nordlander, *Organometallics* 2000, 19, 5568-5574
(15) V. Moberg, R. Duquesne, S. Contaldi, O. Röhrs, J. Nachtigall, L. Damoense, A. T. Hutton, M.Gree, M. Monari, R. Gobetto, M. Haukka and E. Nordlander, *Efficient cluster-based catalysts for asymmetric hydrogenation of* α*-unsaturated carboxylic acids* (manuscript)
(16) W. H. Watson, G. Wu and M. G. Richmond, *Organometallics* 2005, 24, 5431-5439
(17) N. Begum, U. K. Das, H Manzur, G. Hogarth, S. E. Kabir, E. Nordlander and D. Tocher, *Organometallics* 2007, 26, 6462-6472
(18) R. D. Wilson, S. M. Wu, R. A. Love and R. Bau, *Inorganic Chemistry* 1978, 17, 1271
(19) S. P. Tunik, T. S. Pilyugina, I. O. Koshevoy, S. I. Selivanov, M. Haukka and T. A. Pakkanen, *Organometallics* 2004, 23, 568
(20) V. Moberg, P. Homanen, S. Selva, R. Persson, M. Haukka, T. A. Pakkanen, M. Monari and E. Nordlander, *Dalton Transactions* 2006, 279
(21) W. H.Watson, S. Kandala and M. G. Richmond, *Journal of Chemical Crystallography*, vol. 36, No. 10, October 2006, 607
(22) R. A. Sanchez-Delgado, A. Andriollo, J. Puga and G. Martin, *Inorganic Chemistry* 1987, 26, 1867-1870

Table 1. Crystal data for cluster 1.

Identification code	1	
Empirical formula	$C_{62}H_{51}F_{12}FeO_{10}Os_4P_2$	
Formula weight	2062.62	
Temperature	100(2) K	
Wavelength	0.71073 Å	
Crystal system	Monoclinic	
Space group	$P2_1$	
Unit cell dimensions	a = 14.4131(13) Å	α= 90°.
	b = 10.7685(9) Å	β= 94.904(4)°.
	c = 21.041(2) Å	γ = 90°.
Volume	3253.8(5) Å^3	
Z	2	
Density (calculated)	2.105 Mg/m^3	
Absorption coefficient	8.138 mm^{-1}	
Crystal size	0.23 x 0.08 x 0.04 mm^3	
Theta range for data collection	2.98 to 25.02°.	
Index ranges	-17<=h<=17, -12<=k<=12, -24<=l<=25	
Reflections collected	26468	
Independent reflections	10016 [R(int) = 0.0979]	
Completeness to theta = 25.02°	94.0 %	
Absorption correction	Semi-empirical from equivalents	
Max. and min. transmission	0.7528 and 0.2507	
Refinement method	Full-matrix least-squares on F^2	
Data / restraints / parameters	10016 / 586 / 822	
Goodness-of-fit on F^2	1.032	
Final R indices [I>2sigma(I)]	R1 = 0.0588, wR2 = 0.1268	
R indices (all data)	R1 = 0.0896, wR2 = 0.1424	
Absolute structure parameter	0.056(16)	
Largest diff. peak and hole	2.422 and -1.514 e.Å^{-3}	